

A Versatile and Efficient Method to Isolate DNA–Polymer Conjugates

Nico Alleva, Katharina Eigen, David Y. W. Ng,* and Tanja Weil*



Cite This: *ACS Macro Lett.* 2023, 12, 1257–1263



Read Online

ACCESS |



Metrics & More

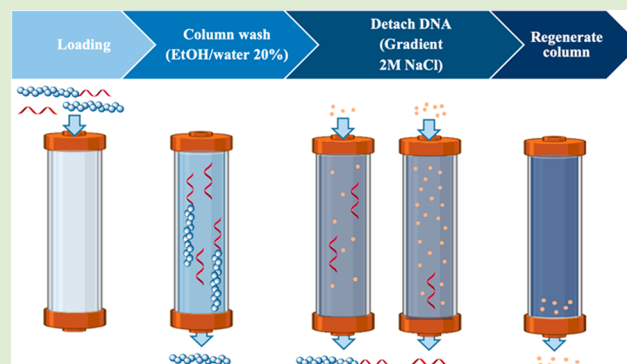


Article Recommendations



Supporting Information

ABSTRACT: We present a facile and adaptable method to purify and isolate DNA–polymer conjugates from different uncharged homo, random, or block copolymer families. Anion exchange chromatography is used to separate the reaction solution and retrieve the excess unreacted polymer and oligonucleotide. The stationary phase has a high efficiency (25 nmol of DNA per run), facilitating the purification of large batches without compromising the peak shape and resolution. To demonstrate the versatility of this method, different types of polymers, including acrylates, methacrylates, and acrylamides containing hydrophilic and hydrophobic blocks, were purified with high yields. Additionally, DNA–polymer conjugates with various DNA block lengths were also successfully purified, further highlighting the broad applicability of this method.



DNA–polymer conjugates have seen a significant expansion in recent years due to the increasing accessibility of DNA, resulting in seminal developments ranging from gene therapy^{1,2} to drug delivery^{3–6} and biosensing.^{7–9} Exploiting the fidelity of DNA technology, they can be used to construct sophisticated shapes and patterns that are only a few nanometers in size, leading to new possibilities for the design and construction of precision nanoscale devices.^{10,11} Furthermore, functional polymer or polymer-coated DNA architectures lead to an enhanced cellular uptake, thereby increasing pharmaceutical applications, for instance as drug carriers.^{12–14} Additionally, by varying the length and composition, they can provide diverse architectures including micelles, vesicles, and tubes.¹⁵ The individual control over the polymer and DNA length, composition, and chemical handles enables broad engineering of conjugate properties for targeted applications.^{14,16}

To prepare DNA–polymer conjugates, the *grafting-to* method is commonly used, which involves using excess amounts of the less expensive polymer to achieve high conversion rates.^{10,17–19} However, this often leads to the challenge of removing the unreacted polymer after the reaction. Because of the high amount of free polymer and the amphiphilic nature of the conjugates, spin filtration with molecular weight cutoffs often results in long purification times and major product loss.¹⁰ Other methods such as reversed-phase high performance liquid chromatography (HPLC) easily reach their capacity limits, requiring extensive optimization of the stationary and mobile phases according to different polymer scaffolds and molecular weights. Alternatively, size exclusion chromatography (SEC) is particularly inefficient for

smaller DNA blocks and the often amphiphilic nature of the conjugates.²⁰ As such, the full integration of polymer science into DNA nanotechnology has not been fully realized due to these pervasive challenges.

To address this limitation, we expand existing approaches of purifying DNA–polymer conjugates with strong anion exchange chromatography,^{21,22} explore its broad applicability toward DNA lengths, different polymer scaffolds, and molecular weights, and compare it with other techniques like HPLC, SEC, and spin filtration. The strategy of this method relies on the negative charge of the DNA block to interact with the positively charged stationary phase. Excess uncharged polymer moves freely through the column and is eluted. Subsequent change in the mobile phase with a gradient of NaCl solution is used to elute DNA containing molecules and allows separation of the DNA–polymer conjugate from minor amounts of unreacted oligonucleotide. Within this method, polymers of three different polymer families (acrylates, acrylamides, and methacrylates) with molecular weight between 9 and 48 kDa were purified as well as conjugates with different DNA block lengths (10, 19, and 40 bases).

Adopting the *grafting-to* strategy, the polymer block is synthesized using polymerization techniques via reversible

Received: June 20, 2023

Accepted: August 29, 2023

Published: September 1, 2023



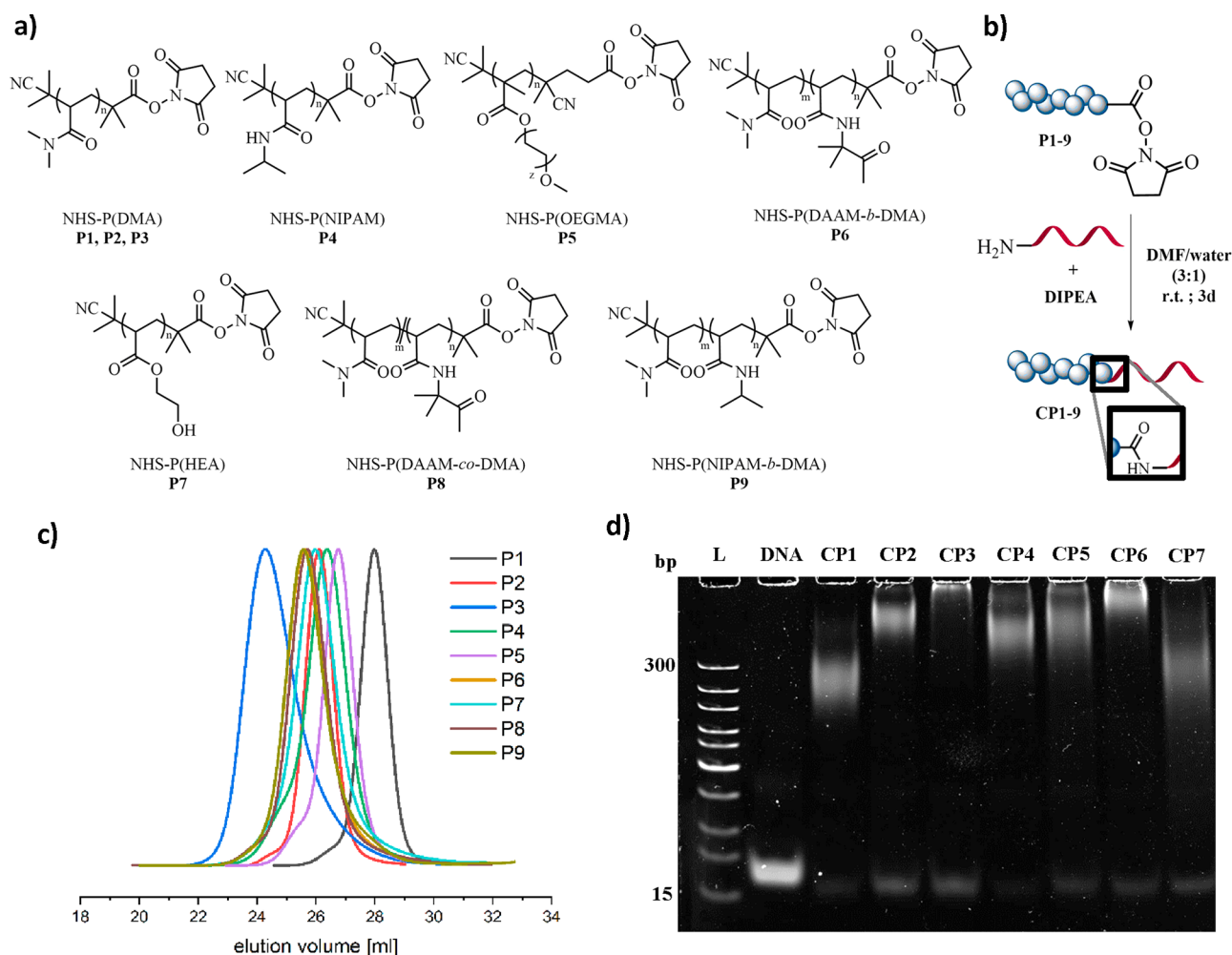


Figure 1. (a) Chemical structure of the NHS polymers used for coupling with the respective DNA. Synthesized via RAFT. (b) General reaction scheme of the NHS coupling to an amine-functionalized oligonucleotide. (c) Elution diagrams of the NHS polymers P1–P9 as measured by DMF SEC using poly(methyl methacrylate) (PMMA) as standard. (d) PAGE gel of the obtained reaction solutions after coupling P1–P7 to 19-base-long oligonucleotide. L: DNA ladder; DNA: used 19-base-long oligonucleotide; CP1–CP7 respective coupling reaction solution of P1–P7. Using SYBR Gold for staining (2 \times).

addition–fragmentation chain transfer (RAFT), which incorporates a functional end-group. Subsequently, the polymer is covalently attached to a complementary functional group on the DNA block. In this case, the strategy was performed using NH₂-functionalized oligonucleotide and NHS-activated polymers prepared by RAFT polymerization.¹⁰ The coupling was performed in a DMF/water (3:1) mixture using 50 equiv of the polymer, with DIPEA as an auxiliary base (Figure 1b). The reaction solution was analyzed using polyacrylamide gel electrophoresis (PAGE) to confirm the formation of the DNA–polymer conjugate and to monitor remaining oligonucleotides (Figures 1d and S22). Using the general conditions above, polymers (P(DMA), P1, 9.6 kDa; P(DMA), P2, 22 kDa; P(DMA), P3, 48 kDa; P(NIPAM), P4, 21 kDa; P(OEGMA), P5, 21 kDa; P(DAAM-*b*-DMA), P6, 26 kDa; P(HEA), P7, 22 kDa; P(DAAM-*co*-DMA) P8, 26 kDa; P(NIPAM-*b*-DMA) P9, 30 kDa) and DNA of various lengths (SDNA, 10 base long; DNA, 19 base long; LDNA, 40 base long) were prepared and coupled. P(DMA) (P1–P3) with varying molecular weights was selected to establish a reliable method and to investigate the impact of polymer block length on the conjugation efficiency. P(NIPAM) (P4) and P(HEA) (P7) were employed to demonstrate how changes in the

properties of the polymer block, specifically hydrophilicity and hydrophobicity, affect the method. The brush-like P(OEGMA) (P5) represents a sterically demanding polymer which potentially influences the binding to the stationary phase. Block copolymers P(DAAM-*b*-DMA) (P6) and P(NIPAM-*b*-DMA) (P9) as well as random copolymer P(DAAM-*co*-DMA) (P8) were also included to demonstrate the robustness of the technique toward complex polymer designs. Additionally, DNA block lengths were varied to show the ease of method adaptation caused by charge and differences in hydrophilicity.

Following polymer to DNA coupling, DMF and DIPEA were removed via spin filtration, and the obtained solution was diluted with water to a final volume of 2 mL, from which 1 mL (25 nmol of DNA) is loaded onto the column (Cytiva HiRes Q 5/50; 5 \times 50 mm² bed dimensions). The purification method contains several steps to prepare/equilibrate the column, separate the components of the reaction solution, and elute them fractionwise (Figure S1). Detection at 260 nm during purification takes into consideration the characteristic absorption of DNA.²³ Additionally, as the polymer absorbs mostly at 240 nm, it is also tracked simultaneously (Figure S2). To prepare the column, the stationary phase is initially washed and equilibrated with water (flow rate: 0.7 mL/min; 5 CV;

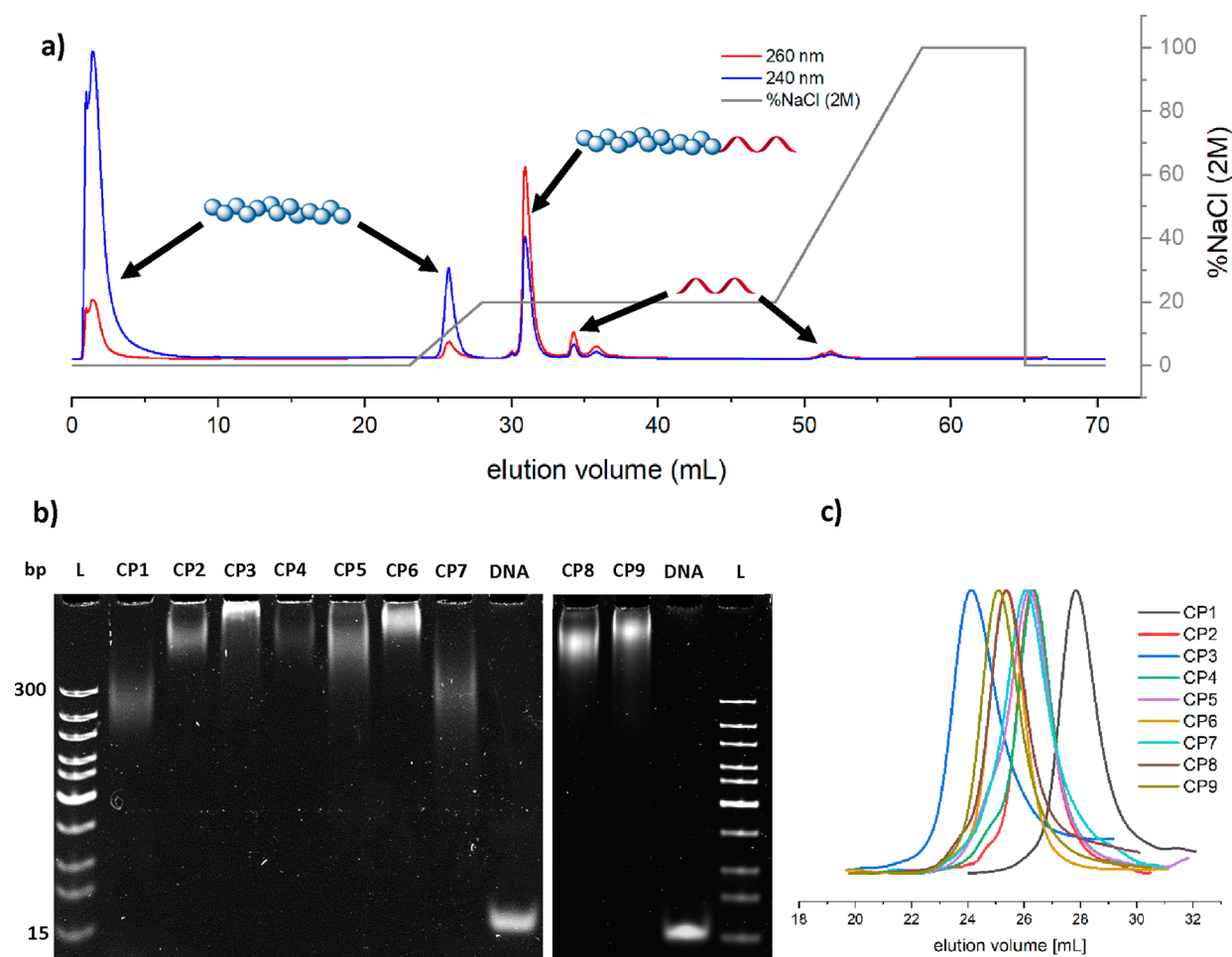


Figure 2. (a) Elution diagram of the CP2 reaction solution run with contemporaneous detection of absorbance at 240 nm (polymer block) and 260 nm (oligonucleotide block). (b) PAGE gel electrophoresis of the respective purified conjugates CP1–CP9. L: DNA ladder; CP1–CP9: respective pure conjugates; DNA: 19-base oligonucleotide as comparison. Stained with SYBR Gold (2 \times). (c) Elution diagrams of the conjugates CP1–CP9 measured by DMF SEC using poly(methyl methacrylate) (PMMA) as standard.

Figure S3) before loading with the diluted reaction solution (Figure S4). Both DNA and the DNA–polymer conjugate are negatively charged, allowing the molecules to bind to the positively charged resin.²⁴ The sample loading is achieved via a 1 mL sample loop and applying 3 mL of water as the loading volume. Subsequently, the column is washed with EtOH/water (20% EtOH, v/v, 20 CV) to remove the unbound, excess free polymer from the solution (Figure S5). Next, stepwise elution is performed by applying a NaCl gradient to control the separation of the bound components (Figure S6). Post elution, the column is washed with 2 M NaCl solution to remove any remaining bound components (Figure S7). Finally, the stationary phase is equilibrated with pure water, and a new run can begin (Figure S8). Because of the charged resin's high binding affinity towards DNA, 25 nmol of DNA per run can be purified without a loss of resolution or purity of the conjugate, despite the small size of the column.

The versatility of the method was demonstrated using NHS-functionalized polymers from three different monomer families (acrylates, methacrylates, and acrylamides) coupled to the 19-base oligonucleotide (Figure 1a). First, using DMA as the scaffold, the polymer length of P(DMA) was varied, comprising a short (P(DMA) \sim 9.6 kDa; P1), middle (P(DMA) \sim 22 kDa; P2), and a longer (P(DMA) \sim 48 kDa; P3) chain to test if the purification remained robust. The

elution diagram for the DNA–polymer conjugate CP2 (Figure 2a) indicates that during loading and washing most of the polymer was successfully removed from the column. Subsequently, the eluent was changed to a gradient of NaCl (0–2 M) solution. As the NaCl solution concentration increases from 0 to 0.4 M, further unbound polymer was eluted from the column. At 0.4 M NaCl, the mobile phase was held isocratic to elute the DNA–polymer conjugate followed by the unreacted DNA oligonucleotide. Thereafter, gradient elution from 0.4 to 2 M NaCl was implemented to regenerate the stationary phase, removing any remaining bound components. Surprisingly, the elution diagrams (Figures 2a and S9–S10) showed no significant changes during purification of the corresponding DNA–polymer conjugates CP1–CP3 (elution volumes: CP1, 31.3 mL; CP2, 31.0 mL; CP3, 30.3 mL). However, the trend shows that the larger the polymer block, the faster the conjugate elutes. We postulate that as the polymer segment increase in size, its collapsed volume increases correspondingly, which affects the accessibility to the DNA block and lowers the binding affinity to the stationary phase. Characterization of the purified DNA–P(DMA) conjugates via PAGE (Figure 2b) and SEC (Figure 2c) demonstrates the successful isolation. The respective yields range from \sim 67% to quantitative (Table S2).

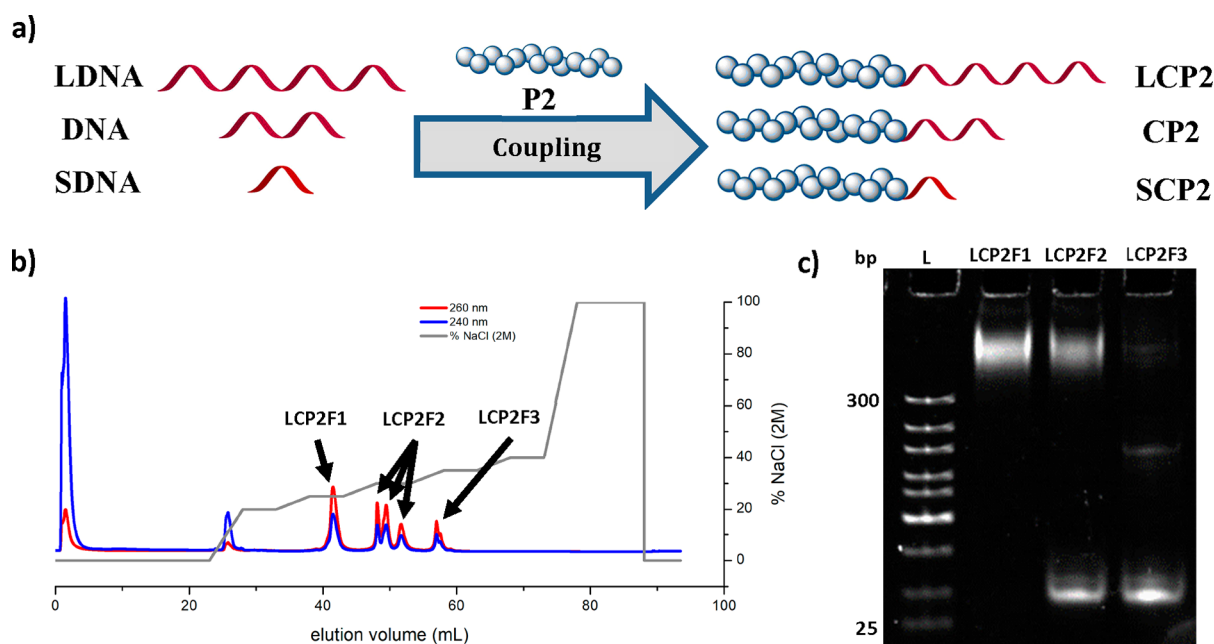


Figure 3. (a) Schematic representation of the coupling reaction of the generated NHS-P(DMA) (**P2**) to the oligonucleotides of different lengths (10, 19, and 40 bases). (b) Elution diagram of the method development profile of the LCP2 reaction solution to find the optimal gradient for the conjugate elution. Here the gradient, starting at 20% was every 5 CV increased by 5% to 40%. (c) PAGE of the LCP2 test run fractions as shown in b). L: DNA ladder; LCP2F1–3: respective fractions. Stained with SYBR Gold (2 \times).

Subsequently, the methodology was applied to a broader range of polymer species, including the more hydrophilic poly(hydroxyl acrylate) (P(HEA), \sim 22 kDa; **P7**) and the more hydrophobic and thermoresponsive^{25–27} poly(*N*-isopropylacrylamide) (P(NIPAM), \sim 21 kDa; **P4**). Despite the varying hydrophilic character of the polymer block, the elution profiles of CP4 and CP7 had no significant impact on the separation efficiency (elution volume: CP4: 31.5 mL, Figure S11; CP7: 31.8 mL, Figure S14). Good to excellent yields were obtained for CP4 (\sim 98%) and CP7 (\sim 70%). The next attempt was to purify more sterically demanding DNA–polymer conjugates by using poly(oligo(ethylene glycol) methacrylate) (P(OEGMA), \sim 21 kDa; **P5**). The elution profile remained unaffected during the purification process (Figure S12). The elution volume of CP5 is 30.7 mL, with a yield of \sim 63% (Table S2). The excess of unreacted brush-like polymer could also be eliminated, as confirmed by SEC (Figure 2c).

The established method was further tested with an amphiphilic block copolymer, which is known to undergo partial phase separation.²⁸ A diacetone acrylamide–DMA block copolymer (P(DAAM-*b*-DMA), \sim 26 kDa; **P6**) and a *N*-isopropylacrylamide–DMA block copolymer (P(NIPAM-*b*-DMA), \sim 30 kDa; **P9**) were synthesized, coupled to DNA to afford CP6 and CP9, and purified using the proposed method. Consistent with the other polymer species tested, no major changes were noted during the purification step, as the elution volume is 31.1 mL for CP6 (Figure S13) and 31.0 mL for CP9 (Figure S17). An isolated yield of \sim 60% for CP6 and \sim 72% for CP9 was obtained, which was similar to that of the brush-like CP5 conjugate. For comparative purposes, a random diacetone acrylamide–DMA copolymer (P(DAAM-*co*-DMA \sim 26 kDa, **P8**) was subjected to coupling and purified, giving an elution time for CP8 of 31.6 mL (Figure S16) and 93% yield. This enhanced yield could be attributed to the reduced phase separation of the polymer during the purification process. These results indicate the method's universal applicability for a

broad range of water-soluble DNA/polymer conjugates with uncharged polymer segments.

Although the variation in polymer lengths and composition had a minimal impact on the chromatographic separation, the length of the DNA segment contributes to the total charge and should therefore influence the elution profile. To this end, we selected 10-base (NH₂-CCACCTACTA; SDNA) and 40-base (NH₂-GAAGATAAAAAACATTTGATTTTTCTCTACCACTACTA; LDNA) oligonucleotides in addition to the 19-base counterpart (Figure 3a). With the different oligonucleotides, polymer **P2** was used as the model polymer and coupled to the DNA strand via the same NHS chemistry. As an initial assessment, PAGE confirmed the successful reactions (Figure 4a). For the purification of the long DNA–polymer conjugate, we used the same gradient optimized for the 19-base oligonucleotide (Figure S15). However, unlike the 19-base DNA–polymer conjugates, the 40-base counterpart (LCP2) eluted at a high retention volume (51–53 mL) together with the unreacted oligonucleotide at higher NaCl concentrations (0.85–1.2 M). Hence, the gradient was modified in order to resolve the separation. We developed a stepwise gradient method to identify the optimal NaCl concentration for elution (Figure 3b). The individual peak fractions were collected, and PAGE was performed to identify the components (Figure 3c). We found that 0.5 M NaCl was the optimal concentration to selectively elute the conjugate, LCP2. Using this knowledge, the original elution diagram was modified with a gradient run until 0.5 M, which was then held isocratic to successfully separate the conjugate LCP2 from the free oligonucleotide (Figure 4b). Because of the gradient adjustment, which was necessary for LCP2, we applied a similar approach for SCP2 by reducing the gradient to 0.3 M NaCl (Figure 4d), resulting in pure conjugate as verified via PAGE gel analysis (Figure 4e). This experiment series demonstrates the method's ease and flexibility in purifying DNA–polymer conjugates with varying DNA block lengths commonly used within DNA nano-

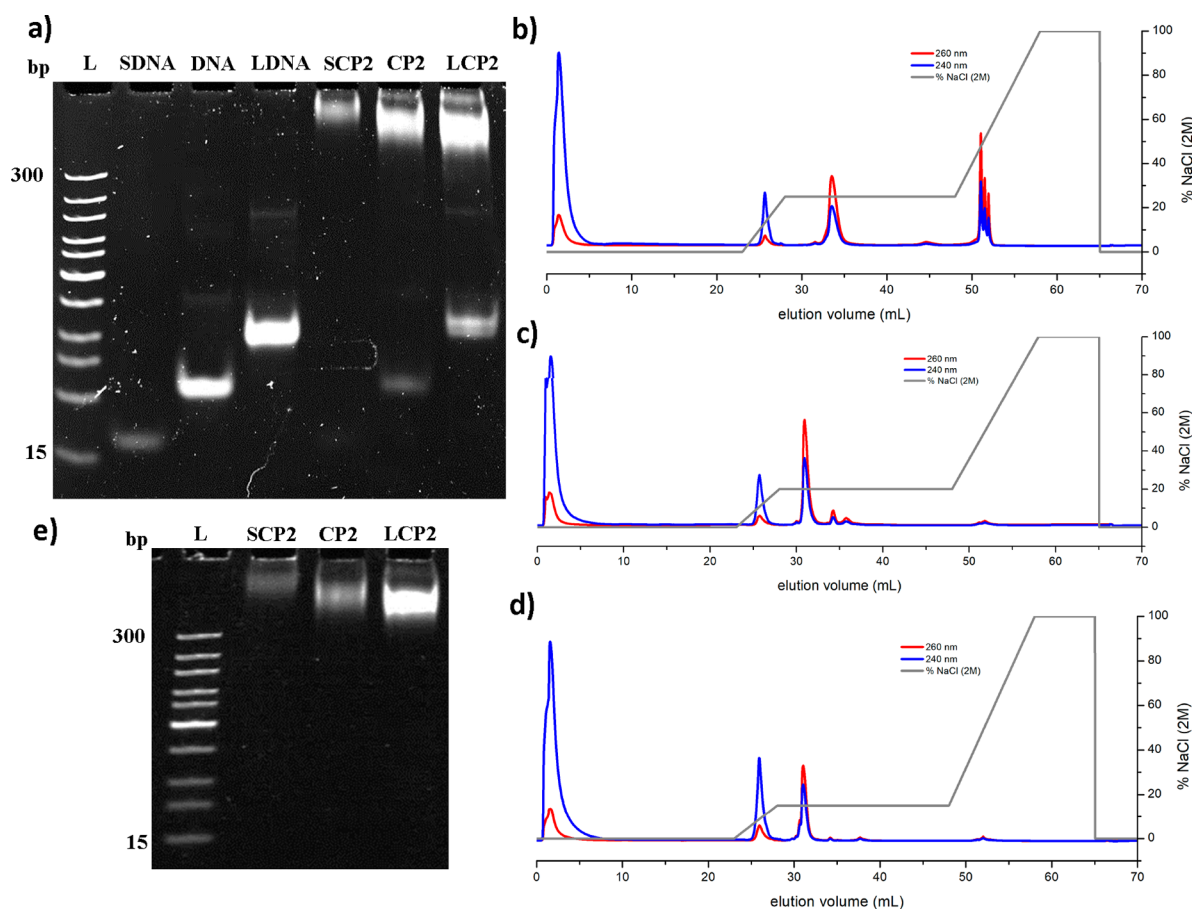


Figure 4. (a) PAGE gel electrophoresis of the pure oligonucleotides and of the reaction solutions after coupling with P2. L: DNA ladder; SDNA: short oligonucleotide (10 base long); DNA: middle oligonucleotide (19 base long); LDNA: long oligonucleotide (40 base long); SCP2: reaction solution of P2 coupled with SDNA; CP2: reaction solution of P2 coupled with DNA; LCP2: reaction solution of P2 coupled with LDNA. Stained with SYBR Gold (2 \times). (b–d) Elution diagram of the whole purification run of the coupling reactions of LCP2, CP2, and SCP2 with P2 with contemporaneous detection of absorbance at 240 nm (polymer block) and 260 nm (oligonucleotide block). (b) LDNA reaction solution. (c) DNA reaction solution. (d) SDNA reaction solution. (e) PAGE gel electrophoresis of the obtained pure conjugates of SCP2, CP2, and LCP2. L: DNA ladder; SCP2/CP2/LCP2: pure conjugate of the respective conjugate was obtained after purification. Stained with SYBR Gold (2 \times).

technology. Based on straightforward method development protocols, further variation of the DNA block lengths can be easily resolved by the NaCl gradient during elution.

Using CP2 as a model DNA–polymer conjugate, we compare our method against analytical scale HPLC and SEC as well as with spin filtration alone. The HPLC studies (Jupiter C18, 5 μ m, 300 Å) were performed first using the reaction mixture of CP2 (8 μ L, 1 nmol), containing 75% (v/v) DMF. Stepwise gradient of acetonitrile/water elution shows several peaks divided into five fractions (F1: 1.25–3.75 mL; F2: 16–16.8 mL; F3: 16.8–17.8 mL; F4: 19–21 mL; F5: 22–22.6 mL) (Figure S18d,e). PAGE gel (Figure S18f) revealed an incomplete separation of the unreacted oligonucleotide and CP2. While F1 shows no conjugate or DNA, F2–F4 include CP2 as well as unreacted oligonucleotide, whereas F5 contains only CP2. Intensity measurements of the bands revealed a yield of 13% for F5 (Table S5). Removal of DMF by spin filtration prior to HPLC separation did not improve the peak resolution (Figure S19). However, the yields of pure fractions F3 and F4 were increased to 45% (Table S5). These results show that even in an analytical scale, purification of CP2 and separation from unreacted oligonucleotide are not optimal. Separate attempts using analytical SEC performed with 8 μ L (1 nmol) reaction solution of CP2 fail to show visible separation

due to the large excess of polymer (50 equiv) present (Figure S20). Purification solely by the spin filtration method (8 cycles) with 10 and 30 kDa molecular weight cutoff were similarly unsuccessful. In each case, the PAGE gel (Figure S21) indicated the continued presence of free oligonucleotide after purification. Overall, these methods present very limited success in isolating pure DNA–polymer conjugates.

The purification efficiency of the method relies on the accessibility of the DNA block to the anionic stationary phase, which is in turn dictated by the length of the polymer block and the steric component of the side-chains. Given a fixed oligonucleotide length of 19 bases, purification efficiency decreases with increasing polymer length (yields: CP1 (~9.6 kDa, quantitative), CP2 (~22 kDa, 96%), CP3 (~48 kDa, 67%). Second, polymers with side-chain bulk such as that of P(OEGMA), CP5, or amphiphilic block copolymers like CP6 reduced the ionic interactions between the oligonucleotide to the column, which in turn lowered the yields. In general, polymers with a molecular weight between 10 and 50 kDa with small, homogeneous side-chains are ideal for this purification method.

In conclusion, we have introduced a versatile and adaptable purification method with high efficiency to purify DNA–polymer conjugates containing various classes of polymers

(acrylates, methacrylates, and acrylamides) and oligonucleotide lengths. Compared to other performed methods like HPLC, spin filtration, or SEC, anion exchange chromatography consistently provides high yields in preparative scale. The purification method is largely independent of the polymer, and even sterically demanding, brush-like DNA–polymer conjugates were isolated successfully. Moreover, complex DNA–polymer conjugates like DNA–P(DAAM-*b*-DMA) and P-(NIPAM-*b*-DMA), with a high tendency to phase separate, could also be purified without loss in resolution. The purification of DNA blocks of different lengths is easily adaptable, which will widen the range of applications of this method in the community. As the unreacted oligonucleotide can also be separated, reuse would also be possible. This reported approach is reliable for water-soluble, noncharged polymer block within DNA–polymer conjugates and can be scaled according to the column dimensions holding the stationary phase. The increased ease of purification and isolation of DNA–polymer conjugates will create greater access and application in nanoscale engineering, biomedicine, and polymer science.

■ ASSOCIATED CONTENT

SI Supporting Information

The Supporting Information is available free of charge at <https://pubs.acs.org/doi/10.1021/acsmacrolett.3c00371>.

Detailed information about the polymer synthesis, the coupling reactions, and the purification method (PDF)

■ AUTHOR INFORMATION

Corresponding Authors

David Y. W. Ng – Max Planck Institute for Polymer Research, 55128 Mainz, Germany; orcid.org/0000-0002-0302-0678; Email: david.ng@mpip-mainz.mpg.de

Tanja Weil – Max Planck Institute for Polymer Research, 55128 Mainz, Germany; orcid.org/0000-0002-5906-7205; Email: weil@mpip-mainz.mpg.de

Authors

Nico Alleva – Max Planck Institute for Polymer Research, 55128 Mainz, Germany

Katharina Eigen – Max Planck Institute for Polymer Research, 55128 Mainz, Germany

Complete contact information is available at: <https://pubs.acs.org/10.1021/acsmacrolett.3c00371>

Author Contributions

CRedit: Nico Alleva conceptualization, data curation, formal analysis, investigation, methodology, supervision, visualization, writing-original draft, writing-review & editing; Katharina Eigen data curation, investigation, writing-review & editing; David Y.W. Ng conceptualization, funding acquisition, investigation, project administration, resources, supervision, writing-original draft, writing-review & editing; Tanja Weil conceptualization, funding acquisition, investigation, project administration, resources, supervision, writing-original draft, writing-review & editing.

Funding

Open access funded by Max Planck Society.

Notes

The authors declare no competing financial interest.

■ ACKNOWLEDGMENTS

The authors acknowledge the financial support by the Deutsche Forschungsgemeinschaft (DFG, German Research Foundation), Project No. 364549901-TRR 234 CataLight (B08), and the Max Planck Society for Open access Funding.

■ REFERENCES

- (1) Ogris, M.; Walker, G.; Blessing, T.; Kirchheis, R.; Wolschek, M.; Wagner, E. Tumor-targeted gene therapy: strategies for the preparation of ligand-polyethylene glycol-polyethylenimine/DNA complexes. *J. Controlled Release* **2003**, *91* (1–2), 173–181.
- (2) Alemdaroglu, F. E.; Alemdaroglu, N. C.; Langguth, P.; Herrmann, A. DNA Block Copolymer Micelles – A Combinatorial Tool for Cancer Nanotechnology. *Adv. Mater.* **2008**, *20* (5), 899–902.
- (3) Kang, H.; Liu, H.; Zhang, X.; Yan, J.; Zhu, Z.; Peng, L.; Yang, H.; Kim, Y.; Tan, W. Photoresponsive DNA-cross-linked hydrogels for controllable release and cancer therapy. *Langmuir* **2011**, *27* (1), 399–408.
- (4) Kedracki, D.; Maroni, P.; Schlaad, H.; Vebert-Nardin, C. Polymer-Aptamer Hybrid Emulsion Templating Yields Bioresponsive Nanocapsules. *Adv. Funct. Mater.* **2014**, *24* (8), 1133–1139.
- (5) Rodríguez-Pulido, A.; Kondrachuk, A. I.; Prusty, D. K.; Gao, J.; Loi, M. A.; Herrmann, A. Light-triggered sequence-specific cargo release from DNA block copolymer-lipid vesicles. *Angew. Chem., Int. Ed.* **2013**, *52* (3), 1008–1012.
- (6) Pokhonenko, O.; Gissot, A.; Valet, B.; Bathany, K.; Thiéry, A.; Barthélémy, P. Lipid oligonucleotide conjugates as responsive nanomaterials for drug delivery. *J. Mater. Chem. B* **2013**, *1* (39), 5329–5334.
- (7) Gibbs, J. M.; Park, S.-J.; Anderson, D. R.; Watson, K. J.; Mirkin, C. A.; Nguyen, S. T. Polymer-DNA hybrids as electrochemical probes for the detection of DNA. *J. Am. Chem. Soc.* **2005**, *127* (4), 1170–1178.
- (8) Chen, T.; Wu, C. S.; Jimenez, E.; Zhu, Z.; Dajac, J. G.; You, M.; Han, D.; Zhang, X.; Tan, W. DNA micelle flares for intracellular mRNA imaging and gene therapy. *Angew. Chem., Int. Ed.* **2013**, *52* (7), 2012–2016.
- (9) Yu, S.; Dong, R.; Chen, J.; Chen, F.; Jiang, W.; Zhou, Y.; Zhu, X.; Yan, D. Synthesis and self-assembly of amphiphilic aptamer-functionalized hyperbranched multiarm copolymers for targeted cancer imaging. *Biomacromolecules* **2014**, *15* (5), 1828–1836.
- (10) Alleva, N.; Winterwerber, P.; Whitfield, C. J.; Ng, D. Y. W.; Weil, T. Nanoscale patterning of polymers on DNA origami. *J. Mater. Chem. B* **2022**, *10* (37), 7512–7517.
- (11) Tokura, Y.; Jiang, Y.; Welle, A.; Stenzel, M. H.; Krzemien, K. M.; Michaelis, J.; Berger, R.; Barner-Kowollik, C.; Wu, Y.; Weil, T. Bottom-Up Fabrication of Nanopatterned Polymers on DNA Origami by In Situ Atom-Transfer Radical Polymerization. *Angew. Chem., Int. Ed.* **2016**, *55*, 5692–5697.
- (12) Winterwerber, P.; Whitfield, C. J.; Ng, D. Y. W.; Weil, T. Multi-Wellenlängen-Photopolymerisation von stabilen Poly(katecholamin)-DNA-Origami-Nanostrukturen. *Angew. Chem., Int. Ed.* **2022**, *61*, No. e202111226.
- (13) Sun, H.; Yang, L.; Thompson, M. P.; Schara, S.; Cao, W.; Choi, W.; Hu, Z.; Zang, N.; Tan, W.; Gianneschi, N. C. Recent Advances in Amphiphilic Polymer-Oligonucleotide Nanomaterials via Living/Controlled Polymerization Technologies. *Bioconjugate Chem.* **2019**, *30* (7), 1889–1904.
- (14) Whitfield, C. J.; Zhang, M.; Winterwerber, P.; Wu, Y.; Ng, D. Y. W.; Weil, T. Functional DNA-Polymer Conjugates. *Chem. Rev.* **2021**, *121*, 11030–11084.
- (15) Peterson, A. M.; Heemstra, J. M. Controlling self-assembly of DNA-polymer conjugates for applications in imaging and drug delivery. *Wiley Interdiscip. Rev.: Nanomed. Nanobiotechnol* **2015**, *7*, 282–297.

(16) Lueckerath, T.; Strauch, T.; Koynov, K.; Barner-Kowollik, C.; Ng, D. Y. W.; Weil, T. DNA-Polymer Conjugates by Photoinduced RAFT Polymerization. *Biomacromolecules* **2019**, *20*, 212–221.

(17) Peng, L.; Wu, C. S.; You, M.; Han, D.; Chen, Y.; Fu, T.; Ye, M.; Tan, W. Engineering and Applications of DNA-Grafting Polymer Materials. *Chem. Sci.* **2013**, *4*, 1928–1938.

(18) Oh, J. S.; Wang, Y.; Pine, D. J.; Yi, G.-R. High-Density PEO-*b*-DNA Brushes on Polymer Particles for Colloidal Superstructures. *Chem. Mater.* **2015**, *27*, 8337–8344.

(19) Hansson, S.; Trouillet, V.; Tischer, T.; Goldmann, A. S.; Carlmark, A.; Barner-Kowollik, C.; Malmström, E. Grafting efficiency of synthetic polymers onto biomaterials: a comparative study of grafting-from versus grafting-to. *Biomacromolecules* **2013**, *14*, 64–74.

(20) Rubner, M. M.; Achatz, D. E.; Mader, H. S.; Stolwijk, J. A.; Wegener, J.; Harms, G. S.; Wolfbeis, O. S.; Wagenknecht, H.-A. DNA “Nanolamps”: “Clicked” DNA Conjugates with Photon Upconverting Nanoparticles as Highly Emissive Biomaterial. *ChemPlusChem*. **2012**, *77*, 129–134.

(21) Zimmermann, J.; Kwak, M.; Musser, A. J.; Herrmann, A. Amphiphilic DNA Block Copolymers: Nucleic Acid-Polymer Hybrid Materials for Diagnostics and Biomedicine. In *Bioconjugation Protocols*; Humana Press: 2011; pp 239–266.

(22) Kwak, M.; Gao, J.; Prusty, D. K.; Musser, A. J.; Markov, V. A.; Tombros, N.; Stuart, M. C. A.; Browne, W. R.; Boekema, E. J.; ten Brinke, G.; Jonkman, H. T.; van Wees, B. J.; Loi, M. A.; Herrmann, A. DNA Block Copolymer Doing It All: From Selection to Self-Assembly of Semiconducting Carbon Nanotubes. *Angew. Chem., Int. Ed.* **2011**, *50* (14), 3206–3210.

(23) Gallagher, S. R.; Desjardins, P. R. Quantitation of DNA and RNA with absorption and fluorescence spectroscopy. *Curr. Protoc. Mol. Biol.* **2006**, *76*, Appendix 3, Appendix 3D.

(24) Budelier, K.; Schorr, J. Purification of DNA by anion-exchange chromatography. *Curr. Protoc. Mol. Biol.* **1998**, Chapter 2, Unit 2.1B.

(25) Murata, M.; Kaku, W.; Anada, T.; Soh, N.; Katayama, Y.; Maeda, M. Thermo responsive DNA/Polymer Conjugate for Intelligent Antisense Strategy. *Chem. Lett.* **2003**, *32*, 266–267.

(26) Feng, C.; Zhu, T.; Jiang, Z.; Ren, C.; Ma, Y. Temperature-regulated non-monotonic behavior of DNA immobilization on poly(*N*-isopropylacrylamide) (PNIPAm)-grafted surface. *Colloids Surf., A* **2022**, *640*, No. 128507.

(27) Yang, T.; Fu, J.; Zheng, S.; Yao, H.; Jin, Y.; Lu, Y.; Liu, H. Biomolecular logic devices based on stimuli-responsive PNIPAM-DNA film electrodes and bioelectrocatalysis of natural DNA with Ru(bpy)₃²⁺ as mediator. *Biosens. Bioelectron.* **2018**, *108*, 62–68.

(28) Lueckerath, T.; Koynov, K.; Loescher, S.; Whitfield, C. J.; Nuhn, L.; Walther, A.; Barner-Kowollik, C.; Ng, D. Y. W.; Weil, T. DNA-Polymer Nanostructures by RAFT Polymerization and Polymerization-Induced Self-Assembly. *Angew. Chem., Int. Ed.* **2020**, *59*, 15474–15479.

Recommended by ACS

Regulation of Interfacial Anchoring Orientation of Anisotropic Nanodumbbells

Hyunwoo Jang, Myung Chul Choi, *et al.*

SEPTEMBER 11, 2023
ACS MACRO LETTERS

READ 

Anti-inflammatory IL-8 Regulation via an Advanced Drug Delivery System at the Oral Mucosa

Maren Witt, Henrik Dommisch, *et al.*

MAY 22, 2023
ACS APPLIED BIO MATERIALS

READ 

Machine Learning Understands Knotted Polymers

Anna Braghetto, Enzo Orlandini, *et al.*

MARCH 24, 2023
MACROMOLECULES

READ 

Effects of Microfluidic Shear on the Plasmid DNA Structure: Implications for Polymeric Gene Delivery Vectors

Lucas J. Andrew, Matthew G. Moffitt, *et al.*

AUGUST 08, 2023
LANGMUIR

READ 

Get More Suggestions >